Bioorganic & Medicinal Chemistry 19 (2011) 2529–2540

Contents lists available at ScienceDirect

Bioorganic & Medicinal Chemistry

journal homepage: www.elsevier.com/locate/bmc

Synthesis and characterization of a cell-permeable bimodal contrast agent targeting β-galactosidase

Aneta Keliris [a,*], Thomas Ziegler [b], Ritu Mishra [a,†], Rolf Pohmann [a], Martin G. Sauer [c], Kamil Ugurbil [a,‡], Jörn Engelmann [a,*]

[a] Max Planck Institute for Biological Cybernetics, Spemannstrasse 41, Tüebingen, Germany
[b] Institute of Organic Chemistry, University of Tuebingen, Auf der Morgenstelle 18, Tüebingen, Germany
[c] Pediatric Hematology & Oncology, Hannover Medical School, Carl-Neuberg-Str. 1, Hannover, Germany

ARTICLE INFO

Article history:
Received 22 September 2010
Revised 5 February 2011
Accepted 9 March 2011
Available online 13 March 2011

Keywords:
β-D-Galactopyranose
Solid phase synthesis
Gadolinium complex
Cellular imaging
Intracellular MRI contrast agent

ABSTRACT

Noninvasive monitoring of intracellular targets such as enzymes, receptors, or mRNA by means of magnetic resonance imaging (MRI) is increasingly gaining relevance in various research areas. A vital prerequisite for their visualization is the development of cell-permeable imaging probes, which can specifically interact with the target that characterizes the cellular or molecular process of interest. Here, we describe a dual-labeled probe, Gd-DOTA-k(FR)-Gal-CPP, designed to report the presence of intracellular β-galactosidase (β-gal) enzyme by MRI. This conjugate consists of a galactose based core serving as cleavable spacer, incorporated between the cell-penetrating peptide D-Tat$_{49-57}$ and reporter moieties (Gd-DOTA, fluorescein (FR)). We employed a facile building block approach to obtain our bimodal probe, Gd-DOTA-k(FR)-Gal-CPP. This strategy involved the preparation of the building blocks and their subsequent assembly using Fmoc-mediated solid phase synthesis, followed by the complexation of ligand **14** with $GdCl_3$. Gd-DOTA-k(FR)-Gal-CPP showed a considerably higher relaxivity enhancement ($16.8 \pm 0.6\ mM^{-1}\ s^{-1}$, 123 MHz, ~21 °C) relative to the commercial Gd-DOTA ($4.0 \pm 0.12\ mM^{-1}\ s^{-1}$, 123 MHz, ~21 °C). The activation of Gd-DOTA-k(FR)-Gal-CPP was based on a cellular retention strategy that required enzymatic cleavage of the delivery vector from galactose moiety following the cell internalization to achieve a prolonged accumulation of the reporter components (Gd-DOTA/FR) in the β-gal expressing cells. Cellular uptake of Gd-DOTA-k(FR)-Gal-CPP in β-gal expressing C6/LacZ and enzyme deficient parental C6 rat glioma cells was confirmed by fluorescence spectroscopy, MR imaging and ICP-AES measurements. All methods showed higher accumulation of measured reporters in C6/LacZ cells compared to enzyme deficient parental C6 cells. Fluorescence microscopy of cells labeled with Gd-DOTA-k(FR)-Gal-CPP indicated a predominantly vesicular localization of the green fluorescent conjugate around cell nuclei. This cellular distribution was most likely responsible for the observed non-specific background signal in the enzyme deficient C6 cells. Even though the specific accumulation of our bimodal probe has to be further improved, it could be already used for cell imaging by MRI and optical modalities.

1. Introduction

Molecular imaging is one of the most dynamically evolving research fields aimed at providing tools for noninvasive, quantitative visualization of fundamental molecular and cellular processes in vivo.[1] Of many clinically essential targets, enzymes are enticing tags for the monitoring of biological events taking place inside the cell. These biocatalysts can serve as specific indicators of disease processes[2,3] and remain popular as reporter molecules for revealing gene expression in biological systems.[4,5] To detect enzyme activity, and hence indirectly gene expression, specific imaging probes are required, which upon conversion produce a characteristic signal measurable by the respective imaging modality. Although mainly optical and nuclear-based approaches have thus far been used for visualization of marker enzyme activity, the contribution of magnetic resonance imaging (MRI) has been increasing over the years. The vast potential of MRI for molecular imaging applications derives from its ability to produce images of opaque organisms noninvasively, at high spatial and temporal resolution and without the use of ionizing radiation.

Basically, MR images are generated by using the NMR signal of water molecules, the intensity of which depends on the relaxation

* Corresponding authors. Tel.: +49 7071 601 704; fax: +49 7071 601 702.
E-mail addresses: aneta.brud@tuebingen.mpg.de (A. Keliris), joern.engelmann@tuebingen.mpg.de (J. Engelmann).
† Present address: Dept. for Biological & Biomedical Sciences, Durham University, Durham, UK.
‡ Present address: Center for Magnetic Resonance Research, Dept. of Radiology, University of Minnesota, Minneapolis, USA.

0968-0896/$ - see front matter © 2011 Elsevier Ltd. All rights reserved.
doi:10.1016/j.bmc.2011.03.023

times (T_1-longitudinal, T_2-transverse) and density of water within a given volume. To enhance MR image contrast in the region of interest being examined, contrast agents (CAs) are commonly applied as imaging probes for MRI. These imaging agents function by accelerating relaxation times of nearby water molecule protons,[6] where their efficacy for inducing such changes is defined by the term 'relaxivity' ($r_{i\,=\,1,2}$).[7] The majority of CAs nowadays employed in clinical practice are based on the paramagnetic gadolinium metal ion (Gd^{3+}) caged within the cavity of a poly(amino carboxylate) ligand. The chelating of Gd^{3+} prevents the toxicity of this metal ion while still permitting the efficient transmission of its paramagnetic effect by the rapid exchange of coordinated water with the bulk solvent. Clinically employed CAs are mostly non-specific and restricted to the extracellular space. Although useful for providing anatomical information, such CAs are incapable of reporting on actual biochemical events themselves (i.e., gene expression and enzyme activity). Therefore, the development of a new generation of highly specific CAs is a vital prerequisite for research in areas aiming at in vivo monitoring of enzyme location and activity by means of MRI. Over the last decade, many efforts were made to devise enzyme-sensing MRI CAs. In general, the mechanism of their activation, leading to a change in their relaxivity via modulation of water hydration number (q) or rotational correlation time (τ_r), was driven by the enzyme-catalyzed formation or cleavage of chemical bonds. Accordingly, alterations such as increasing the q number (r_1 is linearly proportional to q) or slowing down the molecular tumbling rate by increasing the size (longer τ_r) would translate to elevated relaxivity of the Gd^{3+}-complexes. Recent developments contributing towards the creation of enzyme-responsive CAs were initiated with the synthesis of β-EgadMe.[8] This probe was designed to report on β-galactosidase activity, an enzyme encoded by the bacterial *LacZ* reporter gene commonly used for tracking gene expression. The authors used a modulation of q in the inner coordination sphere of the Gd^{3+}-chelate, occurring upon cleavage of the galactose moiety by β-gal, to achieve r_1 changes and thereby MR image contrast enhancement. However, due to its lack of transmembrane permeability, β-EgadMe had to be introduced into the cells by microinjection. A different approach for obtaining enzyme-hydrolysable MRI CAs explored the changes of rotational correlation time (τ_r) through enzyme-controlled modulation of the affinity of the imaging probe for proteins.[9–11] In this case, the enzymatically cleavable moiety is introduced into the protein binding unit to prevent its strong interactions in the absence of enzyme. Thus, upon enzymatic reaction, cleavage of the masking group results in the subsequent binding of the fast tumbling Gd^{3+}-complex to proteins to yield slowly tumbling molecular adducts with higher relaxivity. Together with developments in generating enzyme-hydrolysable MRI CAs, other groups utilized an opposite activation mechanism involving chemical bond formation specifically mediated by target enzymes (i.e., polymerases or oxidoreductases).[10–12] In this instance, the Gd^{3+}-complex bears a moiety which can be specifically oxidized by a certain enzyme to generate reactive product species that subsequently oligomerize in situ to produce slowly rotating larger molecules with higher relaxivity. Although the examples mentioned above demonstrate the feasibility of monitoring enzymatic activity, and thereby visualization of gene expression by MRI, the field is still in its infancy.[13] A decisive constraint on the existing enzyme-responsive MRI CAs regarding their applicability for in vivo monitoring of intracellular enzyme activity, is clearly their lack of efficient cell membrane permeability. Thus, further advances are required to facilitate the optimal translation of such enzyme-based approaches to in vivo models.

With the aim of devising an enzyme-activated MRI CA capable of crossing cell membranes, we synthesized and evaluated the model contrast agent Gd-DOTA-k(FR)-Gal-CPP (Fig. 1) targeting

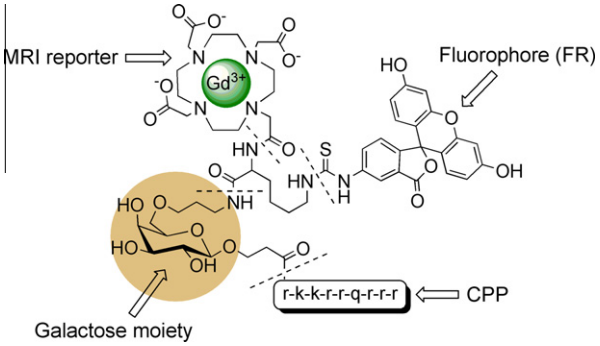

Figure 1. Schematic structure of Gd-DOTA-k(FR)-Gal-CPP. The dashed lines separate the building blocks.

β-galactosidase. In this CA, a galactose moiety (Gal) serving as the enzymatically cleavable linker was inserted between the cell-penetrating peptide (CPP) D-$Tat_{49–57}$ and the Gd^{3+}-based MRI reporter moiety, which is a derivative of Gd-DOTA chelate. The enzymatic activation of this CA following cellular uptake would require enzymatic cleavage of the transporting peptide and subsequent cellular entrapment of the MRI reporter component only in *LacZ*-expressing cells, thereby leading to signal amplification. Thus, the unconverted CA should effectively efflux from cells in the absence of the target enzyme. To exploit the enzymatic cleavage reaction occurring at the anomeric center of the sugar unit, D-$Tat_{49–57}$ was incorporated at the C-1 position of galactose. The MRI imaging reporter was introduced at the C-6 position to maintain enzymatic activity.[14,15] Hydroxyls at C-2, C-3, and C-4 remained unsubstituted because they are essential for binding of galactose moiety to the active site of enzyme and catalytic hydrolysis at anomeric center.[16] To enable the detection of specific cellular retention also by optical imaging, we integrated a fluorescein moiety (FR) into the structure of Gd-DOTA-k(FR)-Gal-CPP. We have chosen D-amino acids for synthesis of the CPP, D-$Tat_{49–57}$, (making it stable to proteases) to ensure that the observed intracellular accumulation of MRI and FR imaging moieties resulted from enzymatic reaction on the sugar and not from peptide degradation. This activation–retention strategy via enzyme-mediated activation had proven successful for radionuclide imaging of reporter gene expression.[17] Here, we present efficient synthesis and physicochemical evaluation of this bimodal, cell membrane-permeable, β-gal-targeting probe. In addition, in vitro assays were performed using β-gal-positive and enzyme deficient cells for the assessment of translocation and specific retention of Gd-DOTA-k(FR)-Gal-CPP inside target-containing cells.

2. Results and discussion

2.1. Synthesis of Gd-DOTA-k(FR)-Gal-CPP

The bimodal probe Gd-DOTA-k(FR)-Gal-CPP (Fig. 1) was obtained using a facile building block strategy, which involved the preparation of basic segments and then linking them together by Fmoc-mediated solid phase synthesis (SPS). We started with the synthesis of the Fmoc-protected galactose derivative **11** (Scheme 1) serving as the key building block for our CA. This monosaccharide was designed in such a way that would enable the efficient incorporation of D-$Tat_{49–57}$ and the DOTA ligand/FR moiety at its respective 1-O and 6-O positions during sequential synthesis on a polymeric support. We based the synthesis of **11** mainly on transformations, which involved thiogalactosides, because these versatile and robust glycosyl donors allow a wide scope of synthetic manipulations. Accordingly, the thiophenyl galactose donor **1**

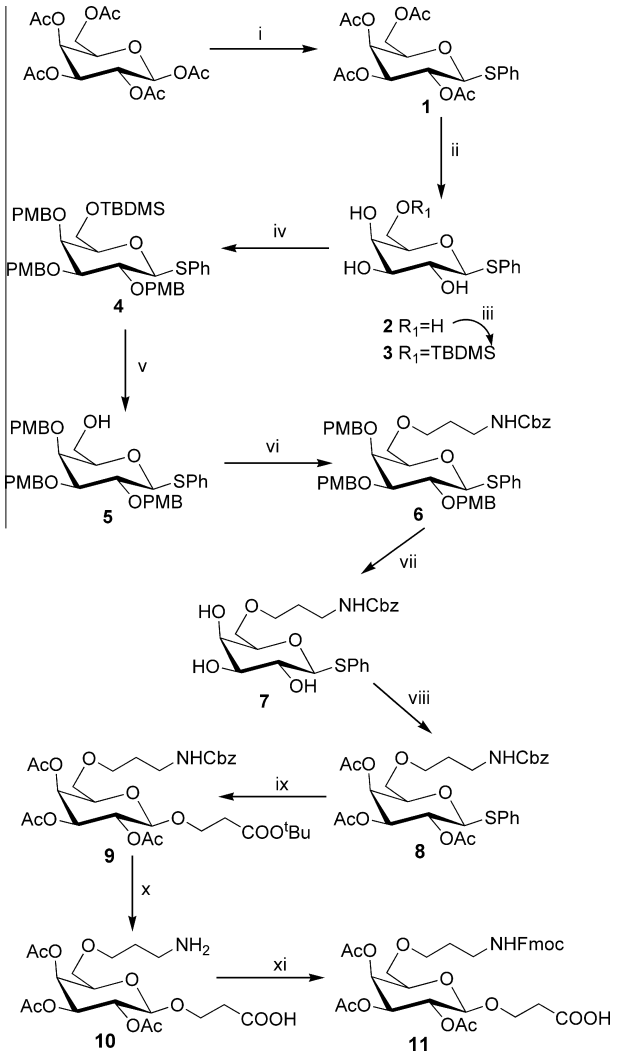

Scheme 1. Synthesis of building block **11**. Reagents and conditions: (i) PhSH, $BF_3{\cdot}Et_2O$, DCM; (ii) $NaOH_{cat.}$, MeOH; (iii) pyridine, Et_3N, TBDMSCl, 0 °C to rt; (iv) NaH, PMBBr, DMF, 0 °C to rt; (v) 1 M TBAF/THF, THF; (vi) $Br(CH_2)_3NHCbz$, NaH, DMF, 0 °C to rt; (vii) DDQ, H_2O/DCM (1:30), rt; (viii) Ac_2O, pyridine; (ix) $Br(CH_2)_2COO^tBu$, NBS, TMSOTf, DCM, −50 °C; (x) (a) DCM/TFA 1:1; (b) H_2/Pd, EtOH; (xi) Fmoc-OSu, Na_2CO_3, DCM, water.

was prepared with a 70% yield using a commercially available penta-*O*-acetyl-β-D-galactopyranoside as the starting material.[18] Following quantitative O-deacetylation, the primary hydroxyl group was silylated with *tert*-butyldimethylsilyl chloride in pyridine-triethylamine to furnish **3** (80%). Hydroxyl groups were protected as *p*-methoxybenzyl (PMB) ethers using *p*-methoxybenzyl bromide and NaH in dry DMF. The resulting product **4** was treated with TBAF in THF to give **5** (69%). The PMB ethers introduced as protecting groups facilitated the subsequent incorporation of a propylene spacer linked Cbz-protected amino functionality into the sugar moiety via an ether bond created at the primary hydroxyl group of **5**. So far, examples of mono-alkylation at the 6-O position of galactopyranosides with higher *n*-alkanes ($n \geqslant 3$) are rare in the literature[19–21] and proved to be difficult in several cases.[22] Hence, to obtain our propylene-tethered derivative **6**, we executed the Williamson reaction as the method of ether preparation most commonly used in organic chemistry. Benzyl 3-bromopropylcarbamate[23] and in situ generated monosaccharide alkoxide of **5** were reacted in DMF at room temperature to give **6** at a moderate yield of 45% after purification. As indicated by TLC and LC–ESI-MS, a small amount of substrate **5** was still present in the reaction mixture even after using the longer reaction time of 48 h. Attempts to increase the conversion by elevating the temperature (55 °C), using a different solvent (THF), or an excess of alkylating agent added in several aliquots after certain time periods, failed to improve the overall reaction yield. Thus, of the reaction conditions tested, the etherification method initially applied proved to be the best to provide **6**. At this point the PMB ethers had to be exchanged with acetate esters in order to assist high glycosylation selectivity towards the β-galactoside **9**. Although an efficient acidic cleavage of PMB ethers using 5% or 10% TFA in DCM (v/v) has been reported elsewhere,[24] both conditions failed to provide **7**. In contrast, oxidative cleavage of PMB groups by DDQ yielded **7** at 60%. Next, the free hydroxyl groups were reacted with acetic anhydride in pyridine to give acetate protected **8** (85%). In the following step, *tert*-butyl 3-hydroxypropionate was subjected to glycosylation with the thiogalactose donor **8** using NBS/Me_3SiOTf as an activator.[25] The resulting β-glycosylated product **9**, formation of which was facilitated by the participation of the neighboring 2-*O*-acetyl group, was obtained at a yield of 50%. The cleavage of the *tert*-butyl ester in **9** with TFA/DCM (1:1) occurred concomitantly with the partial hydrolysis of the Cbz-protecting group. The removal of Cbz was completed by catalytic hydrogenation over Pd/C at 2 bar of hydrogen to yield the intermediate **10**. Finally, the amino group was protected in the reaction of **10** with Fmoc succinimide (Fmoc-OSu) to give the desired building block **11** at a yield of 64%.

We proceeded further with the manual SPS of conjugate **13** as presented in Scheme 2. First, the side chain protected peptide D-$Tat_{49–57}$ ($r_{(Pbf)}k_{(Boc)}k_{(Boc)}r_{(Pbf)}r_{(Pbf)}q_{(Trt)}r_{(Pbf)}r_{(Pbf)}r_{(Pbf)}$) was synthesized on pre-loaded Wang resin. Thereafter, the monosaccharide **11** (3 equiv), activated with HATU (3 equiv)/DIPEA (6 equiv) in DMF, was coupled to the N-amino terminus of the peptide. This step was followed by Fmoc deprotection and conjugation of a Fmoc/Dde protected D-lysine (Fmoc-D-$k_{(Dde)}$-OH) to the amino functionality on the sugar moiety. The attached lysine residue served as a linker for the incorporation of the macrocyclic chelate **12**[26] (DOTA (t-Bu)$_3$) and fluorescein at its respective primary amino groups. After **12** was coupled to the α-NH_2 group of the side chain protected lysine, the Dde group was removed by treatment with 2% hydrazine hydrate in DMF. Subsequently, the fluorophore was introduced at the ε-NH_2 group of lysine in a reaction with fluorescein isothiocyanate (FITC) (4 equiv) and DIPEA (8 equiv) in DMF for 12 h. Finally, the entire molecule was cleaved off the polymeric support using TFA/TIPS/*m*-cresol/water with the simultaneous deprotection of all acid-labile protecting groups of the amino acid side chains as well as *tert*-butyl esters on the macrocyclic chelator. Subsequent O-deacetylation of released conjugate **13** proved to be challenging. Our initial attempts to remove the acetates by hydrazinolysis, prior to release of the molecule from resin,[27] led to decomposition of the O-glycosidic linkage under these acidic conditions. Therefore, deprotection of the acetate esters, which are known to indirectly stabilize the acid-labile bonds,[28] was performed in solution following the detachment of conjugate **13** from the polymeric support. Commonly used procedures such as Zemplén deprotection or treatment with methanolic ammonia were tested. However, under the conditions employed, only an incomplete O-deacetylation of **13** was observed leading to a main product containing a single acetyl group as revealed by LC–ESI-MS analysis. The observed resistance to deprotection might be associated with the previously reported difficulties in cleaving the acetate ester at 4-OH of galactose moieties in polyfunctional systems due to steric hindrance.[29] Finally, treatment of **13** with hydrazine hydrate in MeOH (1:6 v/v)[30] for 12 h was found to be optimal to generate **14**. Metalation of this ligand with gadolinium was accomplished by adding $GdCl_3$ (0.9 equiv) to a solution of **14** (1 equiv) in ultrapure water. Chelation was completed after stirring at room temperature for 72 h, as monitored by LC–ESI-MS. The

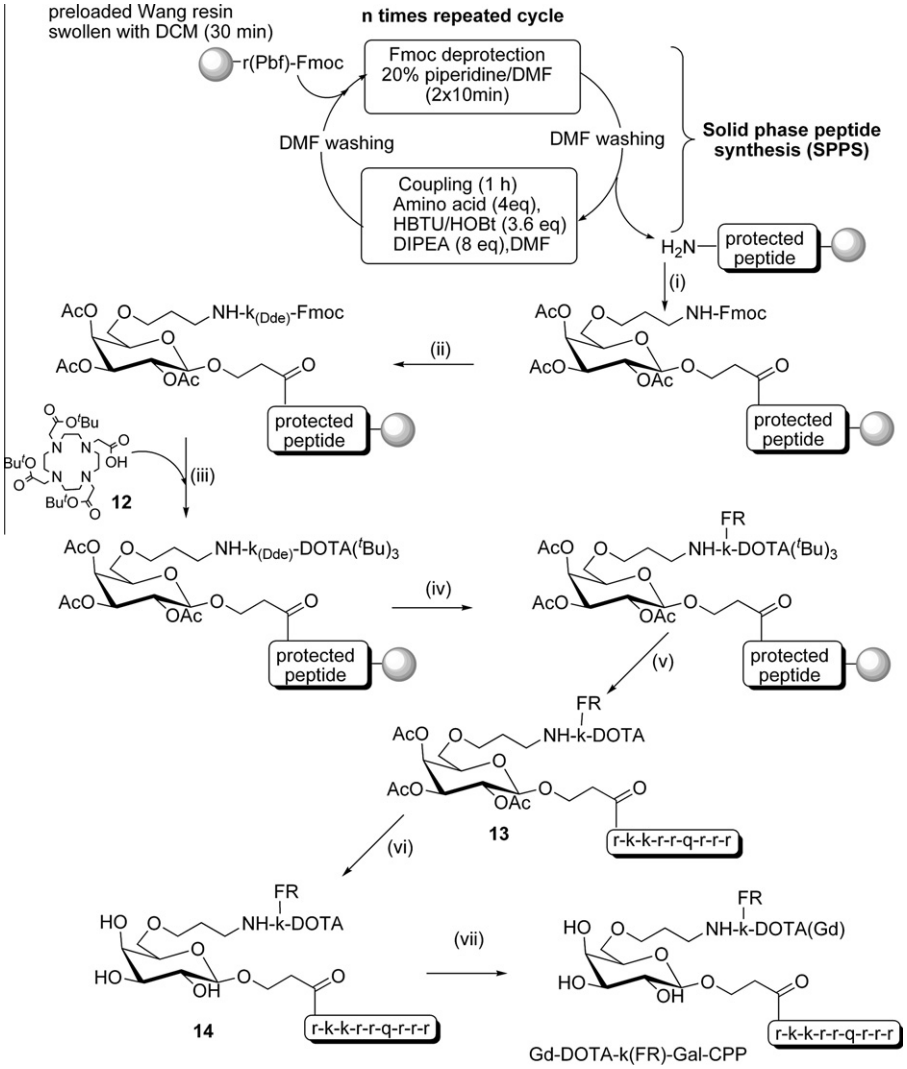

Scheme 2. Synthesis of Gd-DOTA-k(FR)-Gal-CPP. Reagents and conditions: (i) **11**, HATU, DIPEA, DMF, 3 h; (ii) Fmoc-Lys(Dde)-OH, HATU, DIPEA, DMF, 3 h; (iii) DOTA-(t-Bu)$_3$, HATU, DMF, 24 h; (iv) (a) 2% hydrazine hydrate, DMF, 2 × 4 min; (b) FITC, DIPEA, DMF, 12 h; (v) TFA/m-cresol/TIPS/H_2O (90:5:2.5:2.5), 4 h; (vi) hydrazine hydrate/MeOH (1:6 v/v), 12 h; (viii) $GdCl_3 \cdot 6H_2O$, 40 °C/12 h, rt 3 days.

absence of free Gd^{3+} metal ions was confirmed by a competitive assay with DTPA (see Section 4). The crude product was purified by RP-HPLC, dialyzed and lyophilized to yield the desired Gd-DOTA-k(FR)-Gal-CPP, the structure of which was verified by ESI-MS. Hence, the building block approach presented here, which involved different branches of chemistry, proved to be a viable synthetic strategy for devising a bimodal Gd-DOTA-k(FR)-Gal-CPP conjugate.

2.2. Longitudinal relaxivity

The efficacy of Gd-DOTA-k(FR)-Gal-CPP to shorten the water proton relaxation time T_1 was studied at a proton Larmor frequency of 123 MHz at room temperature (~ 21 °C). The r_1 of Gd-DOTA-k(FR)-Gal-CPP in water (16.8 ± 0.6 mM^{-1} s^{-1}) was substantially higher than that of Gd-DOTA (4.0 ± 0.12 mM^{-1} s^{-1}) measured under the same conditions. It is well known that conjugation of bulky molecules (i.e., peptides,[31] proteins[32] or dendrimers[33]) to small Gd-DOTA like complexes reduces their molecular tumbling rate, increases the rotational correlation time (τ_r), and consequently yields MRI probes with elevated relaxivity.[34] However, the grafting of small Gd^{3+} complexes to large macromolecules is not always associated with an effective increase of τ_r for such constructs. Fast and independent local motions of Gd^{3+} containing segments attached to macromolecules can significantly diminish an expected increase of relaxivity for slow rotating high molecular weight conjugates.[35] Thus an increased relaxivity is more likely in case that the fast internal motions of attached Gd^{3+} chelates are restricted.[36] We presume that the observed high longitudinal relaxivity of Gd-DOTA-k(FR)-Gal-CPP was obtained as result of effective increase in global τ_r as a consequence of the higher molecular weight and restricted local motion of the Gd^{3+} chelate moiety. The latter is believed to be an effect of two mainly contributing factors. First, the influence on the local motions might originate from the steric hindrance created by the neighbored fluorophore in the close spatial vicinity of the Gd^{3+} chelate moiety. We assume that a second contribution to slow rotational dynamics of Gd-DOTA-k(FR)-Gal-CCP might be given by the slowed down rotation of the Gd^{3+} chelate moiety due to its coupling at the α-amino group attached to the sterically crowded secondary α-carbon of lysine linker. In order to explore the impact of the structural arrangement in close vicinity of Gd^{3+} chelate on the measured relaxivity, we synthesized a second conjugate, Gd-DOTA-Gal-k(FR)-CPP, shown in Figure 2 (for the synthetic details, see Section 4). The rational for the design of this molecule was to

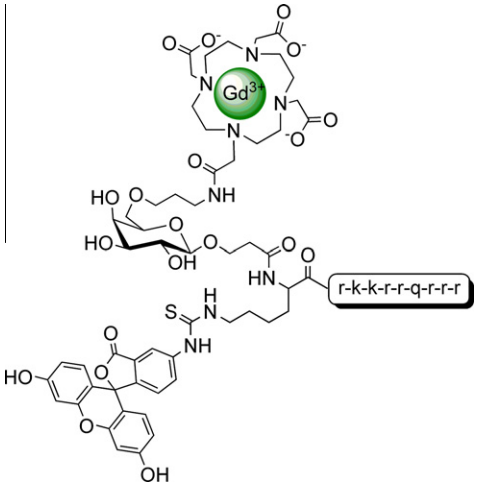

Figure 2. Schematic structure of Gd-DOTA-Gal-k(FR)-CPP.

reduce steric hindrance nearby the Gd^{3+} chelate and thus allow faster local motions by moving the lysine linker with fluorescein to the peptide segment of the conjugate. Accordingly, the Gd-DOTA chelate was directly attached to the aminopropyl spacer of the galactose core whereas the lysine-FR spacer was inserted between the galactose moiety and D-Tat_{49-57} peptide. With this rearrangement we expected decrease in relaxivity due to the increased internal motions of Gd-DOTA moiety. In fact, the measured relaxivity of Gd-DOTA-Gal-k(FR)-CPP ($10.0 \pm 0.8\ mM^{-1}\ s^{-1}$) was significantly lower compared to r_1 values obtained for Gd-DOTA-k(FR)-Gal-CPP, even though the molecular weight of both CAs was identical. It appears evident, that position of the fluorophore with lysine linker relative to the Gd-DOTA chelate had a considerable influence on the r_1 values of the CAs investigated here. On the other hand, the relaxivity of Gd-DOTA-Gal-k(FR)-CPP was still considerably higher than that of Gd-DOTA itself ($4.0 \pm 0.12\ mM^{-1}\ s^{-1}$) showing the influence of a slowed down tumbling rate with increasing molecular size of conjugates. In agreement with our assumption, increase of molecular weight as well as steric hindrance of the local motions of the Gd^{3+} chelate additively contributed to the slower rotational dynamics of Gd-DOTA-k(FR)-Gal-CPP and thus its markedly elevated relaxivity. However, this phenomenon requires more thorough investigations. Only Gd-DOTA-k(FR)-Gal-CPP, as the more efficient CA, was further examined in cell studies.

2.3. Internalization studies by fluorescence spectroscopy

A vital prerequisite for visualization of intracellular targets is clearly the efficient delivery of imaging probes into the cell. Of the well-known CPPs, Tat basic domain peptides have been exploited extensively for translocation of different molecules across cell membranes.[37] Their efficacy proved to be highly dependent on the size and nature of the transported cargo.[38] In the present study, we used fluorescence spectroscopy to assess the efficiency of internalization as well as specific retention of Gd-DOTA-k(FR)-Gal-CPP in rat glioma cells (C6/LacZ) expressing β-galactosidase. The parental cell line (C6), deficient in the target enzyme, was used in all experiments as a control. Due to the proposed mode of activation for Gd-DOTA-k(FR)-Gal-CPP, after incubation with CA, a stronger fluorescent signal would be expected from C6/LacZ cells compared to the enzyme deficient C6 cell line as a result of enzyme-induced cellular retention of imaging moieties via cleavage of the D-Tat_{49-57} permeation peptide. To test our enzyme targeting probe, both cell types were incubated with different concentrations of Gd-DOTA-k(FR)-Gal-CPP under physiological conditions in complete serum containing culture medium. Cells were treated afterwards with trypan blue to quench external and surface-bound fluorescence as well as fluorescence from cells with disrupted cell membrane integrity.[39] As demonstrated by fluorescence spectroscopy, Gd-DOTA-k(FR)-Gal-CPP was very efficiently transported into the cells in a concentration dependent manner (Fig. 3a) and without inducing cytotoxicity up to 20 μM (data not shown). We selected a long treatment time (18 h) in these experiments, because the efficiency of cellular labeling with CA was notably increased (on average twofold) after prolonged incubation times (data not shown). The high cellular uptake of Gd-DOTA-k(FR)-Gal-CPP was of great importance for the subsequent MRI imaging of cells because of the relatively low sensitivity of MRI, which requires large amounts of CA to be delivered for visualization of intracellular targets. Quantitative results of fluorescence spectroscopy revealed a reproducibly greater fluorescence signal from C6/LacZ cells compared to enzyme deficient C6 cells over the whole range of tested concentrations (Fig. 3a). The largest statistically significant difference in the measured fluorescence be-

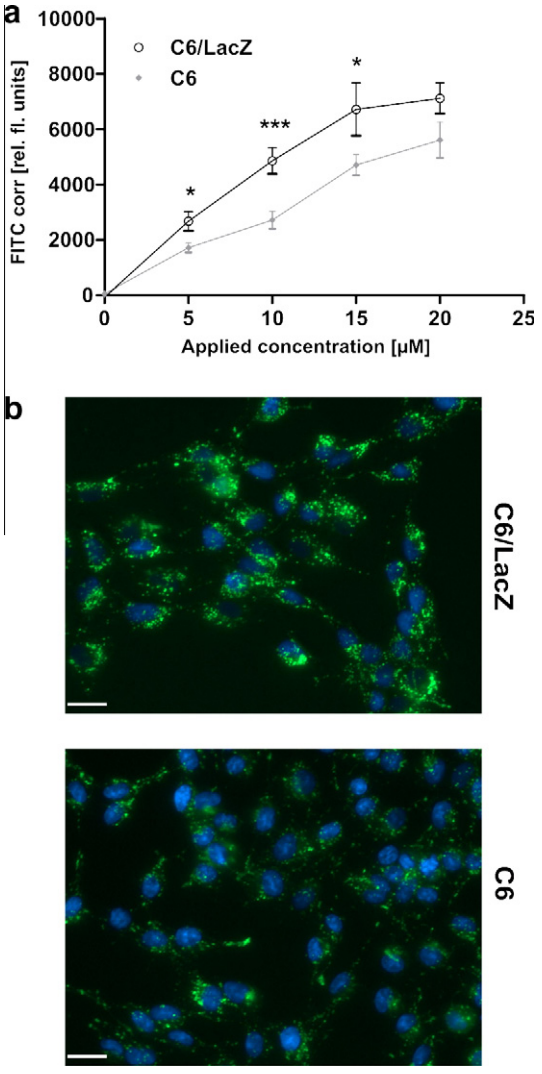

Figure 3. Cellular uptake of Gd-DOTA-k(FR)-Gal-CPP and localization after labeling of C6/LacZ and C6 rat glioma cells in serum containing complete medium for 18 h at 37 °C. External fluorescence was quenched with trypan blue and subsequent washes with HBSS. (a) Fluorescence spectroscopy. Values are means ± SEM (n = 2–4 with six replicates each), $^{*}p$ <0.05, $^{***}p$ <0.001, statistically significantly different compared to C6 cells (Student's t-test). (b) Fluorescence microscopy. Nuclei: blue (Hoe), green (FR fluorescence of contrast agent). The bar represents 20 μM.

tween both cell lines was found at the 10 μM labeling concentration of Gd-DOTA-k(FR)-Gal-CPP. Hence, these data imply that the bimodal probe investigated here showed the expected higher cellular retention in transgenic β-galactosidase expressing cells, despite the presence of strong non-specific fluorescence in enzyme deficient C6 cells.

2.4. Fluorescence microscopy studies

Following fluorescence spectroscopy, we performed fluorescence microscopy with the same cells. The microscopic images of labeled cells showed that green fluorescent conjugate was predominantly localized in vesicles displayed as bright punctuate dots around nuclei (Fig. 3b). The observed cellular distribution pattern might indicate endocytosis as the main route of internalization of Gd-DOTA-k(FR)-Gal-CPP. Endocytosis was recently proposed by other groups as a common translocation mechanism of CPPs.[40] Nonetheless, there are still several uncertainties regarding this mechanism because many factors can radically influence the efficiency of cellular uptake as well as subcellular distribution of permeation peptides with integrated cargos.[38,41] Furthermore, preserved functionality of the CPP-associated cargo also proved to be ambiguous. Reports demonstrating restricted contact of CPP-transported cargo with cytosolic targets due to endosomal encapsulation[42] as well as examples of the opposite, documenting efficient interactions[43,44] can be found in the literature. For example, efficient activation by proteases and cellular retention of cargo transported by Tat only in target-containing cells has been reported[45] proving the successful utilization of this peptide for enzyme targeting approaches.

2.5. MR imaging in cells

To assess the ability of our CA to increase the cellular relaxation rates ($R_{1,cell}$ ($1/T_1$)), we performed spin-lattice relaxation time (T_1) measurements of cells incubated with Gd-DOTA-k(FR)-Gal-CPP using a 3T human MR scanner. A labeling concentration of 10 μM was chosen for the MRI cell studies because of the results of fluorescence spectroscopy showing the largest difference in the cellular accumulation of the imaging probe between β-gal expressing C6/LacZ and deficient of enzyme C6 cells at this concentration of externally applied CA. Accordingly, confluent cultures of C6/LacZ and parental C6 cells were incubated with 10 μM of Gd-DOTA-k(FR)-Gal-CPP for 18 h. Control cells were treated in the same way but without CA in the culture medium. The relaxation rates of the samples were determined in an axial slice through the pellet.

The MR results showed a substantial positive contrast enhancement in C6/LacZ as well as C6 cells after loading with 10 μM of CA (Fig. 4). The used labeling concentration, 10–30 times lower than those typically reported for delivery of CPP coupled Gd-DOTA chelates into cells,[46,47] was sufficient to observe an increase of cell-associated T_1 values. This might be due to the high longitudinal relaxivity of Gd-DOTA-k(FR)-Gal-CPP conjugate (see Section 2.2). The increase of cellular relaxation rates $R_{1,cell}$ ($1/T_1$) of labeled C6/LacZ as well as C6 cells was statistically significant compared to control cells without CA as indicated in Figure 5. A slightly higher increase of $R_{1,cell}$ values was observed in C6/LacZ compared to enzyme deficient C6 cells. However, this difference in $R_{1,cell}$ values was not statistically significant. The gadolinium content in these cells was further quantified by ICP-AES of corresponding cell lysates. The results revealed an about four times higher concentration of gadolinium in β-gal containing C6/LacZ cells (0.85 ± 0.05 Gd fmol/cell) compared to enzyme deficient C6 cells (0.21 ± 0.01 Gd fmol/cell). Hence, our results demonstrated a significantly higher loading of C6/LacZ cells by the MRI reporter compared to C6 cells and remain in agreement with the fluorescence spectroscopy data. However, it is also obvious that the cellular relaxation rate $R_{1,cell}$ of intact cells does not linearly correlate with the internalized gadolinium concentration. The non-significant difference in cellular relaxation rates $R_{1,cell}$ between both cell lines might be ascribed to the lower relaxivity of the smaller residual MRI probe accumulating in C6/LacZ cells upon the cleavage of D-Tat_{49-57} peptide. The converted MRI probe is expected to have faster rotational dynamics compared to parent Gd-DOTA-k(FR)-Gal-CPP conjugate, thereby lower r_1. Therefore, even though the Gd-loading of C6/LacZ cells was much higher compared to C6 cells, the cellular relaxation rate $R_{1,cell}$ would be influenced to a lesser extent by the cleaved probe, and probably in our case not enough to create a substantial difference in $R_{1,cell}$ between both cell lines. Moreover, the predominantly vesicular localization of the dual-labeled probe, observed by fluorescent microscopy, would certainly reduce the dynamic efflux of the uncleaved Gd-DOTA-k(FR)-Gal-CPP, thereby leading to a significant non-specific background signal contributing to the overall signal detected in either cell line. In addition, the largely vesicular distribution of the probe in cells can cause so called relaxation quenching by restricting the number of water molecules which have access to the contrast agent.[48,49] Endosomal entrapment presumably reduced the extent of interactions between cytosolic enzyme and our conjugate. The detected higher accumulation of imaging reporters in C6/LacZ cells suggested, however, that a certain amount of conjugate could escape the vesicles and retained its intended functionality. Examples of maintained biological functionality of endocytically internalized cargo molecules were discussed in the literature.[50,51] El-Andaloussi et al. reported, that entrapped fluorescent cargo molecules could to some extent escape the endosomes and exhibit its biological activity, even though only an exclusively punctuate vesicular distribution was detected in microscopic images. It was stated in several reports that small amounts of cargo released from endosomes could not be detected by microscopy in the presence of the much stronger fluorescence from the vesicles but also because of concentrations below

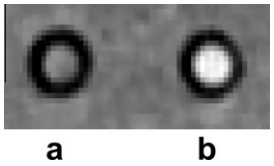

Figure 4. T_1-weighted images of C6/LacZ cells incubated with 10 μM of Gd-DOTA-k(FR)-Gal-CPP for 18 h. (a) Control without contrast agents and b) cells with Gd-DOTA-k(FR)-Gal-CPP.

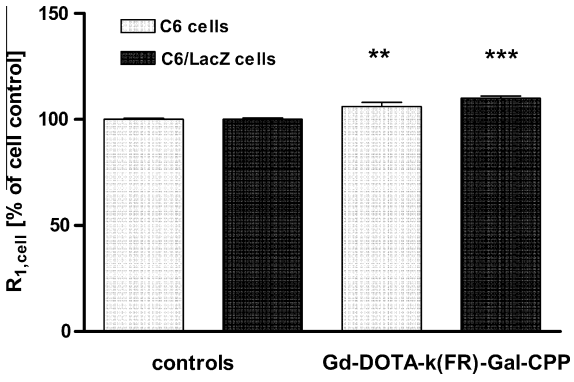

Figure 5. Cellular relaxation rates $R_{1,cell}$ in C6/LacZ and C6 cells after labeling with 10 μM of Gd-DOTA-k(FR)-Gal-CPP for 18 h at 37 °C. Cells were trypsinized, centrifuged and re-suspended in 1.5 ml Eppendorf tubes at 2×10^7 cells/500 μl in complete serum containing medium for MRI studies. Control: cells incubated identically with culture medium without CA. Values are means ± SEM ($n = 2$), $^{**}p < 0.01$, $^{***}p < 0.001$ statistically significantly different compared to respective controls (Student's t-test).

0.2 μM will be masked by autofluorescence.[50,52,53] We assume that the cytosolic localization of our conjugate was not detectable by fluorescence microcopy for the same reasons. Furthermore, the discrepancies in the quantitative measurements from ICP-AES, MR, and optical imaging can be also related to the sensitivity difference between these methods.[54] Nonetheless, all methods showed a tendency for higher loading with imaging reporters in enzyme containing C6/LacZ cells, indicating a specific accumulation of bimodal probe in the presence of the enzymatic target. To improve the interaction of the contrast agent with the cytosolic target, a more efficient release from the vesicles or its direct uptake into the cytoplasm are required. We are currently working on such strategies.[55]

3. Conclusions

In summary, we report the synthesis of a novel dual-labeled imaging probe Gd-DOTA-k(FR)-Gal-CPP, based on a galactose moiety with incorporated Gd-DOTA, FR and transduction (D-Tat$_{49-57}$) moieties. This contrast agent was produced using a multistep building block strategy. Gd-DOTA-k(FR)-Gal-CPP showed a substantial increase of r_1 values compared to the commercially available Gd-DOTA chelate. The insertion position of fluorescein-lysine spacer versus the attachment position of Gd-DOTA chelate was found to have a significant effect on the resultant longitudinal relaxivity values of the synthesized Gd^{3+} complexes. In vitro cell studies revealed that Gd-DOTA-k(FR)-Gal-CPP was very efficiently internalized into cells in a concentration dependent fashion. The higher accumulation of imaging reporters in enzyme containing C6/LacZ cells was observed by fluorescent spectroscopy, MRI and ICP-AES measurements. Nonetheless, structural modifications are still required to circumvent the predominantly vesicular entrapment of the CA investigated here, and these are currently underway. Despite restricted interactions with the target enzyme, we nevertheless developed an efficient cell-permeable bimodal CA, which can be potentially used for cell imaging by MRI as well as optical modalities.

4. Experimental

4.1. General methods

All reagents and solvents were purchased from Acros Organics, Fluka, Sigma–Aldrich or Merck (Germany) and used without further purification unless otherwise stated. Tetraazacyclododecane (cyclen) was obtained from Strem Chemicals (USA). The used Fmoc-protected D-amino acid derivatives (Fmoc-D-Arg(Pbf)-OH, Fmoc-D-Lys(Boc)-OH, Fmoc-D-Gln(Trt)-OH, Fmoc-D-Lys(Dde)-OH), 2-(1*H*-benzotriazol-1-yl)-1,1,3,3-tetramethyluronium hexafluorophosphate (HBTU), and Wang resin pre-loaded with Fmoc/Pbf protected D-arginine (0.4 mmol/g, 100–200 mesh) were obtained from Novabiochem, United Kingdom. 2-(1-*H*-7-Azabenzotriazol-1-yl)-1,1,3,3-tetramethyluronium hexafluorophosphate (HATU) was purchased from McTony (Canada). Dry, anhydrous solvents: DMF, dichloromethane (DCM), acetonitrile (ACN), methanol (MeOH) as Sure-Seal bottles with molecular sieves, *N*,*N*-Diisopropylethylamine (DIPEA), and hydroxybenzotriazole (HOBt) were purchased from Acros Organics (Belgium). Water was purified using a Milli-Q Synthesis purifier (Millipore, Germany). Column chromatography was carried out using silica gel, mesh size 70–230 Å (Merck, Germany). Aluminum sheet silica gel plates with 0.2-mm-thick Silica Gel 60 F_{254} (Merck, Germany) were used to run thin-layer chromatography (TLC). The compounds were visualized by UV_{254} light or charring with 5% H_2SO_4/EtOH (for carbohydrates) or I_2 vapor. Optical rotations $[\alpha]_D$ were measured at 20 °C with a Perkin–Elmer Polarimeter 341 (Perkin–Elmer, Germany) using a 1 dm quartz cell and the concentrations are reported in g/100 ml. Analytical and semi-preparative Reversed-Phase High Performance Liquid Chromatography (RP-HPLC) were performed at room temperature on a Varian PrepStar Instrument (Australia) equipped with PrepStar SD-1 pump heads. UV absorbance was measured using a ProStar 335 photodiode array detector at 214 and 245 nm. Analytical RP-HPLC was performed on a Polaris C_{18}-Ether column (4.6 × 250 mm, particle size 5 μm, particle pore diameter 100 Å; Varian, Germany) and preparative RP-HPLC was performed on a Polaris 5 C_{18}-Ether column (21.2 × 250 mm, 5 μm, 100 Å; Varian, Germany) or Polaris C_8-Ether column (100 × 250 mm, 5 μm, 100 Å). The compounds were purified using one of the following methods. Method 1: a linear gradient was used with the mobile phase starting from 90% of solvent A (0.1% TFA/water), 10% of solvent B (0.1% TFA/acetonitrile) isocratic for 5 min and increased to 60% B over 20 min, moving to 90% B over 3 min, and 90% B isocratic up to 30 min. Method 2: a linear gradient was used with the mobile phase starting from 80% of solvent C (0.05% TFA/water), 10% of solvent D (0.05% TFA/acetonitrile) isocratic for 5 min and increased to 60% D over 20 min, moving to 90% D over 3 min, and 90% D isocratic up to 30 min. The flow rate used for analytical HPLC was 1 ml/min and for a preparative RP-HPLC 4 ml/min or 10 ml/min. All the injected solutions were filtered through a nylon-66 Millipore filter (0.45 mm) prior to purification. Electrospray Ionization-Mass Spectrometry (ESI-MS) spectra were measured on an SL 1100 system (Agilent, Germany) with ion-trap detection in positive and negative mode. HR-FT-ICR mass spectra were generated on an APEX 2 spectrometer (Bruker Daltonic, Germany) with ESI. Liquid Chromatography–Electrospray Ionization-Mass Spectrometry (LC–ESI-MS) analysis of samples was performed using an in-house system consisting of an analytical RP-HPLC Beckman System Gold LC 126 (Germany) and the ESI-MS SL 1100 system (Agilent, Germany). The LC system was equipped with 508 Autosampler. UV absorbance was measured using UV 168 detector at 214 and 245 nm. RP-HPLC was performed using a Polaris C_{18}-Ether column (4.6 × 250 mm, particle size 5 μm, particle pore diameter 100 Å, Varian, Germany). NMR spectra were recorded on a Bruker Avance II 300 MHz 'Microbay' spectrometer (^{1}H: $CDCl_3$ internal reference at 7.27 ppm, DMSO at 2.5 ppm, TMS at 0 ppm); (^{13}C, 75 MHz: internal reference $CDCl_3$ at 77.0 ppm, DMSO at 39.51 or TMS at 0 ppm). Abbreviations: ps-pseudo-singlet, os-overlapping singlet, pd-pseudo-doublet. All measurements were performed at room temperature. Solvent residual signals in ^{1}H and ^{13}C NMR spectra were assigned based on published data.[56] Proton and carbon signal assignments were confirmed by ^{1}H–^{1}H-COSY and ^{1}H–^{13}C-COSY (HSQC) experiments. Gadolinium concentrations of Gd-DOTA-k(FR)-Gal-CPP, Gd-DOTA-Gal-k(FR)-CPP, and cell lysates were determined at Mikroanalytisches Labor Pascher (Remagen, Germany) by ICP-AES on an Icap 6500 by Thermo Instruments.

4.2. Experimental procedures and spectral data

4.2.1. Phenyl-1-thio-β-D-galactopyranoside (2)

O-Acetyl deprotection of **1** (150 mmol, 66 g) was carried out in dry MeOH (500 ml) in the presence of sodium methoxide. Progress was monitored by TLC (MeOH/ethyl acetate 1:9, R_f = 0.25). After completion, the reaction mixture was neutralized with Dowex®50Wx8-100 ion-exchange resin (pH ~6), filtered, and concentrated to give **2** (40 g, 98%) in the form of an oil**.** The spectral data were consistent with that reported in the literature.[18]

4.2.2. Phenyl 6-(*O*-*tert*-butyldimethylsilyl)-1-thio-β-D-galactopyranoside (3)

To a solution of **2** (78.96 mmol, 21.5 g) in dry pyridine (310 ml) *tert*-butyldimethylsilyl chloride (TBDMSCl) (118.4 mmol, 17.84 g)

was added portionwise, followed by triethylamine addition at −10 °C over 20 min under nitrogen. The reaction mixture was stirred at −10 °C for 1 h, slowly warmed up to room temperature and stirred for the next 20 h until the starting material was consumed, as monitored by TLC (MeOH/ethyl acetate 9:1, R_f = 0.9). The mixture was diluted with DCM (400 ml), poured into ice-cold water and extracted with DCM (4×). The combined organic layers were washed with saturated aqueous $NaHCO_3$, brine, dried over Na_2SO_4, filtered, and concentrated. The organic residue was purified by column chromatography using hexane/ethyl acetate to yield **3** as a yellow viscous oil (80%, 24.42 g). $[\alpha]_D^{20}$ = −45.6 (*c* 0.8, MeOH). ^{1}H NMR (300 MHz, DMSO-d_6): δ = 0.05, 0.07 (2s, 2 × 3H, SiCH_3), 0.9 (s, 9H, C(CH_3)$_3$, 3.37–3.50 (m, 2H, H-2, H-3), 3.52–3.64 (m, 1H, H-5), 3.68–3.77 (m, 3H, H-6, H-4), 4.54 (pd, 1H, OH), 4.64 (d, 1H, J_{1-2} = 9.1 Hz, H-1), 4.97 (pd, 1H, OH), 5.18 (pd, 1H, OH), 7.20–7.36 (m, 3H, Ar-*H*), 7.45–7.51 (m, 2H, Ar-*H*). ^{13}C NMR (75 MHz, DMSO-d_6): δ = −5.28, −5.44 (SiCH_3), 17.98 (*C*(CH_3)$_3$), 25.81 (C(CH_3)$_3$), 62.89 (C-6), 68.50, 69.16, 74.56 (C-4, C-2, C-3), 79.04 (C-5), 87.80 (C-1), 126.03 128.71, 129.07, 135.72 (ArH). HRMS (EI) (+) for $C_{18}H_{30}O_5SSi$: [[M+Na]$^+_{(found)}$ = 409.14752, M+Na]$^+_{(calcd)}$ = 409.14754.

4.2.3. Phenyl 2,3,4-tri-*O*-(4-methoxybenzyl)-6-*O*-(*tert*-butyldimethylsiloxypropyl)-1-thio-β-D-galactopyranoside (4)

To a solution of **3** (32.8 mmol, 12.64 g) and 4-methoxybenzyl bromide (115 mmol, 23 g, 16.6 ml) in anhydrous DMF (400 ml), sodium hydride (115 mmol, 4.6 g, 60% dispersion in mineral oil) was added at −10 °C. The reaction mixture was stirred at −10 °C for 30 min and the next 4 h at room temperature. The progress of the reaction was monitored by TLC (hexane/ethyl acetate 1:1, R_f = 0.7). The reaction mixture was cooled to 0 °C, diluted with cold water and extracted with diethyl ether (3×), followed by ethyl acetate extraction (2×). The combined organic layers were washed with water and brine, dried over Na_2SO_4, filtered, and concentrated under vacuum. The residue was purified by column chromatography on silica gel using hexane/ethyl acetate to yield **4** as a yellowish, viscous oil (70%, 17.1 g). $[\alpha]_D^{20}$ = +1.6 (*c* 1.0, $CHCl_3$). ^{1}H NMR (300 MHz, $CDCl_3$): δ = 0.02, 0.03 (2s, 6H, SiCH_3), 0.87 (s, 9H, C(CH_3)$_3$)), 3.40 (pt, 1H, H-5, *J* = 6.52), 3.54 (dd, 1H, H-3, J_{3-2} = 11.9 Hz, J_{3-4} = 2.64 Hz), 3.58–3.76 (m, 2H, H-6), 3.80, 3.82 (os, 9H, CH_3), 3.85–3.95 (m, 2H, H-4, H-2), 4.55 (d, 1H, *J* = 11.4 Hz), 4.60 (d, 1H, H-1, J_{1-2} = 9.63 Hz), 4.62–4.76 (os, 4H, OCH_2), 4.90 (d, 1H, *J* = 10.95 Hz), 6.8–6.92 (m, 6H, Ar*H*), 7.10–7.25 (m, 3H, Ar*H*), 7.26–7.35 (m,6H, Ar*H*), 7.49–7.51 (m, 2H, Ar*H*). ^{13}C NMR (75 MHz, $CDCl_3$): δ = −5.51, −5.27 (SiCH_3), 18.16 (*C*(CH_3)$_3$), 25.86 (C(CH_3)$_3$), 55.23 (*C*H_3), 61.72 (C-6), 72.44 (OCH_2), 73.14 (C-4), 74.00 (OCH_2), 75.18 (OCH_2), 77.03 (C-2), 78.96 (C-5), 83.92 (C-3), 87.79 (C-1), 113.51, 113.69, 113.77, 126.76, 128.69, 129.19, 129.30, 129.36, 129.92, 130.42, 130.49, 130.63, 131.13, 134.51, 158.99, 159.17, 159.22 (Ar). HRMS (EI) (+) for $C_{42}H_{54}O_8SSi$: [M+Na]$^+_{(found)}$ = 769.32018, [M+Na]$^+_{(calcd)}$ = 769.32009.

4.2.4. Phenyl 2,3,4-tri-*O*-(4-methoxybenzyl)-6-hydroxy-1-thio-β-D-galactopyranoside (5)

A 1 M solution of TBAF in THF (15.6 ml) was added dropwise at 0 °C under nitrogen to a suspension of compound **4** (22.35 mmol, 16.67 g) and pulverized molecular sieves (4 Å) in freshly distilled THF (117 ml). The reaction mixture was allowed to warm up to room temperature (∼1 h) and was stirred for the next 6 h. After completion (monitored by TLC), the reaction mixture was filtered through Celite 545, which was washed thoroughly with ethyl acetate. The collected filtrate was concentrated under vacuum and the residue was re-dissolved in ethyl acetate, washed with saturated aqueous $NaHCO_3$ and water. The organic layer was dried over Na_2SO_4, filtered, and concentrated in vacuo. The crude product was purified on silica gel by column chromatography using hexane/ethyl acetate as eluent (hexane/ethyl acetate 1:1, R_f = 0.49) to yield **5** at 69% as a white foam. $[\alpha]_D^{20}$ = −2.4 (*c* 0.8, $CHCl_3$).^{1}H NMR (300 MHz, $CDCl_3$): δ = 3.35–3.52 (m, 2H, H-5, 1H, H-6), 3.55 (dd, 1H, H-3, J_{3-2} = 9.3 Hz, J_{3-4} = 2.83 Hz), 3.75–3.85 (m, 11H, H-6, CH_3, H-4), 3.90 (t, 1H, H-2, *J* = 9.44 Hz), 4.56 (d, 1H, OCH_2, *J* = 11.52 Hz), 4.62 (d, 1H, H-1, J_{1-2} = 9.63 Hz), 4.65–4.79 (m, 4H, OCH_2), 4.88 (d, 1H, OCH_2, *J* = 11.33 Hz), 6.82–6.94 (m, 6H, ArH), 7.14–7.37 (m, 9H, ArH), 7.48–7.57 (m, 2H, ArH). ^{13}C NMR (75 MHz, $CDCl_3$): δ = 55.23 (*C*H_3), 62.23 (C-6), 72.68 (OCH_2), 72.74 (C-4), 73.64 (OCH_2), 75.26 (OCH_2), 77.23 (C-2), 78.72 (C-5), 83.91 (C-3), 87.75 (C-1), 113.71, 113.73, 113.84, 127.06, 128.79, 129.21, 129.90, 130.27, 130.37, 130.45, 131.37, 134.08, 159.26 (Ar). HRMS (EI) (+) for $C_{36}H_{40}O_8S$: [M+Na]$^+_{(found)}$ = 655.23398, [M+Na]$^+_{(calcd)}$ = 655.23361.

4.2.5. Phenyl 2,3,4-tri-*O*-(4-methoxybenzyl)-6-*O*-(3-benzyloxycarbonylaminopropyl)-1-thio-β-D-galactopyranoside (6)

Sodium hydride (47.6 mmol, 1.9 g, 60% dispersion in mineral oil) was added portionwise at −10 °C to a solution of **5** (14.5 mmol, 9.16 g) in DMF (95 ml) under nitrogen. The reaction mixture was stirred for 30 min at −10 °C and *N*-benzyloxycarbonyl-3-bromopropylamine (58 mmol, 15.8 g) dissolved in DMF (13 ml) was added. Stirring was continued at −10 °C for 30 min and then at room temperature. The progress of the reaction was monitored by TLC. After 24 h the reaction mixture was cooled to 0 °C, MeOH (7 ml) was slowly added to destroy the excess of sodium hydride. The mixture was stirred for 10 min, further diluted with ethyl acetate (250 ml) and poured into ice-cold water. The organic layer was separated and the water layer was extracted with ethyl acetate (3×), DCM (1×). The organic layers were combined, dried over Na_2SO_4, filtered, and concentrated in vacuo. The residue was purified by silica gel column chromatography with hexane/ethyl acetate as eluent (hexane: ethyl acetate 1:1, R_f = 0.6), to give 5.37 g (45%) of **6** as a white viscous oil. $[\alpha]_D^{20}$ = +6.8 (*c* 0.9, $CHCl_3$). ^{1}H NMR (300 MHz, $CDCl_3$): δ = 1.63–1.75 (m, 2H, CH_2NH), 3.1–3.29 (m, 2H, CH_2NH), 3.3–3.65 (m, 5H, H-5, H-6, OCH_2CH$_2$, H-3), 3.7–3.95 (m, 12H, H-6, CH_3, H-2, H-4), 4.54 (d, 1H, OCH_2, *J* = 11.33 Hz), 4.60 (d, 1H, H-1, J_{1-2} = 9.82 Hz), 4.64–4.75 (m, 4H, OCH_2), 4.88 (d, 1H, OCH_2, *J* = 11.33 Hz), 4.95–5.2 (2 os, 3H, PhCH_2, N*H*)), 6.8–6.91 (m, 6H, Ar*H*), 7.1–7.4 (m, 14H, ArH), 7.5–7.6 (m, 2H, Ar*H*). ^{13}C NMR (75 MHz, $CDCl_3$): δ = 22.60 (*C*H_2), 38.86 (*C*H_2NH), 55.22 (*C*H_3), 66.47 (C-6), 69.47, 69.64 (OCH_2CH$_2$, OCH_2Ph) 72.43 (OCH_2),, 73.11 (C-4), 73.87, 75.20 (OCH_2), 77.20 (C-2), 77.30 (C-5), 83.92 (C-3), 87.77 (C-1), 113.55, 113.68, 113.78, 126.93, 128.0, 128.43, 128.69, 129.16, 129.48, 129.89, 130.38, 130.53, 130.81, 131.34, 134.36, 136.61, 156.29, 159.07, 159.17, 159.23 (Ar). HRMS (EI) (+) for $C_{47}H_{53}NO_{10}S$: [M+K]$^+_{(found)}$ = 862.30217, [M+K]$^+_{(calcd)}$ = 862.30218.

4.2.6. Phenyl 6-*O*-(3-benzyloxycarbonylamidopropyl)-1-thio-β-D-galactopyranoside (7)

Compound **6** (6.20 mmol, 5.2 g) was dissolved in DCM (90 ml) and water (3 ml) was added followed by DDQ addition (27.83 mmol, 6.32 g). The mixture was stirred for 24 h at room temperature, diluted with DCM, filtered and washed with saturated aqueous $NaHCO_3$, $Na_2S_2O_3$, and brine. The organic layer was dried over Na_2SO_4, filtered, and concentrated. The residue was purified on silica gel by flash column chromatography using MeOH/DCM as eluent (MeOH/ethyl acetate 1:9, R_f = 0.6) to yield **7** as a white solid (1.7 g, 60%). $[\alpha]_D^{20}$ = −30.2 (*c* 0.9, MeOH). ^{1}H NMR (300 MHz, $CDCl_3$): δ = 1.47–1.85 (m, 2H, CH_2), 3.05–3.52 (m, 4H, CH_2NH, OCH_2CH$_2$), 3.53–3.75 (m, 4H, H-3, H-5, OH), 3.76–4.41 (m, 5H, H-6, H-2, H-4, OH), 4.56 (d, 1H, H-1, J_{1-2} = 9.63 Hz), 5.04 (s, 2H, OCH_2Ph), 5.26 (br s, N*H*), 7.14–7.38 (m, 8H, Ar*H*), 7.45–7.57 (m, 2H, Ar*H*). ^{13}C NMR (75 MHz, $CDCl_3$): δ = 29.72

(CH_2), 38.16 (CH_2NH), 66.64 (OCH_2Ph)), 68.78 (OCH_2CH_2), 68.95 (C-4), 69.55 (C-6), 69.97 (C-2), 74.79, 77.20 (C-5, C-3), 88.66 (C-1), 113.64, 127.53, 128.04, 128.46, 128.86, 131.74, 136.50, 156.64 (Ar). HRMS (EI) (+) for $C_{23}H_{29}NO_7S$: $[M+Na]^+_{(found)}$ = 486.15571, $[M+Na]^+_{(calcd)}$ = 486.15569.

4.2.7. 2,3,4-Tri-*O*-acetyl-6-*O*-(3-benzyloxycarbonylamidopropyl)-1-thio-β-D-galactopyranoside (8)

Pyridine (13 ml) was placed in a flask (under nitrogen), cooled to −10 °C and acetic anhydride (10.7 ml) was added. Compound **7** (1.57 g, 3.4 mmol) was dissolved in 3 ml of pyridine and added dropwise to the pyridine/acetic anhydride mixture at −10 °C. The reaction mixture was allowed to warm up to room temperature and stirred overnight. The progress of the reaction was checked by TLC. After 24 h, the reaction mixture was diluted with ethyl acetate (100 ml) and poured into ice-cold water. The organic layer was separated and the water layer was extracted with ethyl acetate (3×). The organic layers were combined, dried over Na_2SO_4, filtered, and concentrated. The organic residue was purified by column chromatography on silica gel using hexane/ethyl acetate to give **8** (1.7 g, 85%) as a colorless syrup (hexane: ethyl acetate 1:1, R_f = 0.7). $[\alpha]_D^{20}$ = +2.0 (*c* 0.9, $CHCl_3$). ^{1}H NMR (300 MHz, $CDCl_3$): δ = 1.63–1.76 (m, 2H, C*H*$_2$), 1.97, 2.09, 2.11 (3s, 3 × 3H, C*H*$_3$CO), 3.14–3.30 (m, 2H, C*H*$_2$NH), 3.32–3.61 (m, 2H, H-6, 2H, OC*H*$_2$CH$_2$), 3.76–3.87 (m, 1H, H-5), 4.72 (d, 1H, H-1, J_{1-2} = 10 Hz), 4.99–5.18 (m, 4H, H-3, PhC*H*$_2$, N*H*), 5.24 (dd, 1H, H-2, J_{2-1} = 10 Hz, J_{2-3} = 10 Hz), 5.44 (pd, 1H, H-4, J_{3-4} = 3 Hz), 7.24–7.39 (m, 8H, Ar*H*), 7.45–7.53 (m, 2H, Ar*H*). ^{13}C NMR (75 MHz, $CDCl_3$): δ = 20.55, 20.62, 20.81 (COCH3), 29.44 (*C*H$_2$CH$_2$NH), 38.30 (*C*H$_2$NH), 66.41 (PhCH$_2$), 67.49, 67.73 (C-2, C-4), 68.60 (OCH$_2$), 69.22 (C-6), 72.05 (C-3), 77.75 (C-5), 86.59 (C-1), 127.97, 128.86, 132.74, 136.74 (Ar), 156.45 (NHCOO), 169.45, 169.94, 170.34 (CH$_3$CO). HRMS (EI) (+) for $C_{29}H_{35}NO_{10}S$: $[M+K]^+_{(found)}$ = 628.16124, $[M+K]^+_{(calcd)}$ = 628.16133.

4.2.8. 3-(2,3,4-Tri-*O*-acetyl-6-*O*-(3-benzyloxycarbonylamidopropyl))-β-D-galactopyranos-1-yl)-*tert*-butyl propionate (9)

To a solution of **8** (2.6 mmol 1.53 g), in dry DCM (90 ml) under nitrogen *tert*-butyl 3-hydroxypropionate (5.2 mmol, 0.76 g), in DCM (1 ml) and pulverized molecular sieves (4 Å) were added. The reaction mixture was stirred for 1 h at room temperature and then cooled to −50 °C. NBS (6.72 mmol, 1.2 g) was added followed by addition of Me_3SiOTf (0.5 mmol, 0.11 g) and stirring continued for the next 45 min at which time the substrate **8** was fully consumed as detected by TLC. The reaction mixture was diluted with DCM (150 ml), filtered through Celite 545 and washed thoroughly with DCM. The collected filtrate was washed with saturated aqueous $NaHCO_3$, aqueous $Na_2S_2O_3$, brine, and water. The organic layer was dried over Na_2SO_4, filtered, and concentrated in vacuo. The residue was purified using hexane/ethyl acetate as eluent by column chromatography on silica gel (hexane/ethyl acetate 3:1, R_f = 0.45) to give **9** (0.81 g, 50%) as a colorless syrup. $[\alpha]_D^{20}$ = −6.9 (*c* 0.9, $CHCl_3$). ^{1}H NMR (300 MHz, $CDCl_3$): δ = 1.44 (s, 9H, C(C*H*$_3$)$_3$), 1.61–1.84 (m, 2H, C*H*$_2$CH$_2$), 1.97, 2.04, 2.13 (3s, 3 × 3H, C*H*$_3$CO), 2.28–2.62 (m, 2H, C*H*$_2$COO), 3.08–3.63 (m, 6H, C*H*$_2$O, C*H*$_2$NH), 3.67–3.87 (m, 2H, H-5, H-6), 3.93–4.10 (m, 1H, H-6), 4.48 (d, 1H, $J_{1,2}$ = 7.7 Hz, H-1), 5.0 (dd, 1H, H-3, J_{3-2} = 10.4 Hz, J_{3-4} = 3.4 Hz), 5.09 (os, 2H, PhCH$_2$O), 5.11–5.27 (m, 2H, H-2, N*H*), 5.41 (d, 1H, H-4, J_{3-4} = 3.1 Hz), 7.24–7.43 (m, 5H, Ar*H*). ^{13}C NMR (75 MHz, $CDCl_3$): δ = 20.56, 20.65, 20.74 (COCH$_3$), 28.04 (C(CH$_3$)$_3$), 29.43 (CH$_2$), 35. 83 (*C*H$_2$) 38.41 (*C*HNH), 65.45 (*C*H$_2$O$_{C\text{-}6}$), 66.40 (*C*H$_2$O$_{C\text{-}1}$), 67.63 (C-4), 68.47 (C-6), 68.96 (C-2), 69.35 (PhCH$_2$O), 71.01 (C-3), 71.89 (C-5), 80.69 (*C*(CH$_3$)$_3$), 101.30 (C-1), 127.98, 128.01, 128.44 (Ph), 136.77 (Ph), 156.46 (NHCO), 169.45, 170.05, 170.27 (CH$_3$CO), 170.44 (CH$_2$COO). HRMS (EI) (+) for $C_{30}H_{43}NO_{13}$: $[M+NH_4]^+_{(found)}$ = 643.30736 $[M+NH_4]^+_{(calcd)}$ = 643.30727.

4.2.9. 3-((2,3,4-Tri-*O*-acetyl-6-*O*-((*N*-9-fluoroenylmethoxycarbonyl)amino)propyl))-β-D-galactopyranos-1-yl)-propanoic acid (11)

To a solution of **9** (1.27 mmol, 0.56 g) in DCM (24 ml) neat TFA (24 ml) was added at 0 °C and the mixture was stirred at room temperature for 15 h, then co-evaporated with toluene to give a mixture of crude **10** and a partially deprotected intermediate with the remaining Cbz group. The organic residue was dissolved in ethanol (50 ml), 10% Pd/C (0.2 g) and a few drops of formic acid were added (pH ∼4). The reaction mixture was flushed with nitrogen, then with hydrogen and stirred for 8 h under a hydrogen atmosphere (2 bar). After flushing with nitrogen, the solution was filtered by Celite 545, sorely washed with ethanol and concentrated to give crude **10**. This material was dissolved in a mixture of dioxane/water (90 ml, 1:1 v/v) and solid Na_2CO_3 (3.0 mmol, 0.32 g) was added. The reaction mixture was ultrasonicated for 15 min, cooled to 0 °C, Fmoc-OSu (1.9 mmol, 0.64 g) added and stirring continued for the next 6 h. The reaction mixture was acidified with aqueous HCl (pH ∼5), diluted with water and the water layer was extracted with DCM (3×). The organic layer was dried over Na_2SO_4, filtered, and concentrated in vacuo. The organic residue was purified on silica by column chromatography starting with hexane/ethyl acetate (1:1) followed by MeOH/DCM eluent (MeOH/DCM 1:9, R_f = 0.4) to yield 0.5 g (64%) of **11** as a greenish oil. $[\alpha]_D^{20}$ = +2.8 (*c* 1.0, $CHCl_3$). ^{1}H NMR (300 MHz, $CDCl_3$): δ = 1.65–1.8 (m, 2H, C*H*$_2$CH$_2$NH), 1.97, 2.04, 2.14 (3s, 3 × 3H, COC*H*$_3$, 2.53–2.69 (m, 2H, C*H*$_2$COOH), 3.1–3.6 (m, 6H, C*H*$_2$NH, CH$_2$OC*H*$_2$, H$_a$-6, H$_b$-6), 3.75–3.94 (m, 2H, H-5, OC*H*$_2$CH$_2$COOH), 4.0–4.15 (m, 1H, OC*H*$_2$CH$_2$COOH), 4.17–4.29 (pt, 1H, C*H*Fmoc), 4.32–4.57 (m, 3H, OC*H*$_2$Fmoc, H-1), 4.95–5.09 (dd, 1H, J_{3-4} = 3.2 Hz, J_{3-2} = 10.4 Hz, H-3), 5.12–5.22 (dd, 1H, H-2, J_{2-1} = 8.0 Hz, J_{2-3} = 10.4 Hz), 5.3 (s, 1H, NH), 5.42 (pd, 1H, H-4), 7.27–7.35 (t, 2H, Fmoc), 7.36–7.45 (t, 2H, Fmoc), 7.60 (d, 1H, Fmoc), 7.76 (d, 1H, Fmoc). ^{13}C NMR (75 MHz, $CDCl_3$): δ = 20.53, 20.64 (COCH$_3$), 29.36 (*C*H$_2$CH$_2$NH), 34.68 (*C*H$_2$COOH), 38.19 (*C*H$_2$NH), 47.25 (*C*HFmoc), 65.37 (OCH$_2$CH$_2$COOH), 66.36 (NHCOOCH$_2$), 67.64 (C-4), 68.37 (C-6), 68.92 (C-2), 69.09 (CH$_2$OCH$_2$), 70.90 (C-3), 71.90 (C-5), 101.57 (C-1), 119.91, 124.99, 126.98, 127.62, 143.91 (Fmoc), 156.62 (NHCO), 169.61, 170.08, 170.52 (COCH$_3$), 175.19 (COOH). HRMS (EI) (+) for $C_{33}H_{39}NO_{13}$: $[M+K]^+_{(found)}$ = 696.20540, $[M+K]^+_{(calcd)}$ = 696.20530.

4.2.10. Solid phase synthesis of 13

The peptide was synthesized manually using a Heidolph Synthesis 1 synthesizer (Heidolph, Germany) by the Fmoc SPPS method on a pre-loaded polysterene-based Wang resin containing Fmoc/Pbf protected D-arginine (loading 0.4 mmol/g). The resin (0.08 mmol, 200 mg) was initially washed with DCM (2×) and swelled for 30 min in DCM, followed by further washing with DMF (6×). The Fmoc group was removed by treatment with 20% piperidine/DMF (2 × 10 min). The resin was drained and washed with DMF (4×) after each deprotection and coupling step. The D-amino acids were coupled by adding a pre-activated mixture of an appropriate Fmoc-protected D-amino acid (4 equiv) [Fmoc/Boc-D-lysine, Fmoc/Pbf-D-arginine, Fmoc/Trt-D-glutamine], HBTU (3.6 equiv)/HOBt (3.6 equiv) in DMF (2 ml) and DIPEA (8 equiv) and stirring the mixture for 1 h. The Fmoc-protected peptide D-Tat$_{49-57}$ (Fmoc-r$_{(Pbf)}$k$_{(Boc)}$k$_{(Boc)}$r$_{(Pbf)}$r$_{(Pbf)}$q$_{(Trt)}$r$_{(Pbf)}$r$_{(Pbf)}$r$_{(Pbf)}$) was treated with 20% piperidine/DMF and washed thoroughly with DMF (6×). Coupling of the sugar building block **11** was performed by adding a pre-activated solution of Fmoc-protected compound **11** (3 equiv), HATU (3 equiv) in DMF (3 ml) and DIPEA (6 equiv) to the peptide linked resin. After 3 h of coupling under nitrogen atmosphere, the resin was washed with DMF (4×). After Fmoc group deprotection on the sugar moiety, Fmoc-D-Lys(Dde)-OH was coupled to the free amino group of the sugar. The Fmoc-D-Lys(Dde)-OH (4 equiv) and HATU (4 equiv) were dissolved in

DMF (3 ml), DIPEA (8 equiv) was added and the resulting solution was allowed to react for 3 h under nitrogen**.** The Fmoc group was removed by treatment with piperidine and the resin was washed with DMF (4×). Coupling of the DOTA-(t-Bu)$_3$ ester **12** to the α-NH_2 group of lysine was carried out by adding a pre-activated solution of **12** (4 equiv) with HATU (4 equiv) in DMF (3 ml) and DIPEA (8 equiv) to the resin and the reaction was allowed to continue for 24 h under nitrogen. The Dde group of the lysine linker was removed by treatment with 2% hydrazine hydrate in DMF (2 × 4 min) and the fluorophore was coupled to ε-NH_2 group of lysine within 12 h (FITC (4 equiv): DIPEA (8 equiv), DMF (3 ml)). All coupling steps were followed by Kaiser test on the resin to indicate presence (deprotection) or absence (coupling) of free amino groups. The resin was washed with DMF (4×), DCM (4×), and MeOH (6×) and dried under vacuum. The resin attached conjugate was cleaved off the resin with TFA/water/TIPS/m-cresol (90:5:2.5:2.5 v/v/v/v) for 4 h and washed with TFA (2 ml). The crude product was precipitated with cold (−20 °C) *tert*-butyl methyl ether (MTBE). The precipitate was washed with an additional amount of MTBE (2×), centrifuged and re-suspended in neat TFA. After precipitation with cold MTBE and centrifugation, the crude product was dissolved in H_2O/t-BuOH (2:1 v/v) and lyophilized to afford crude **13** as orange powder. This conjugate was purified by semi-preparative RP-HPLC using method 1 (Polaris 5 ether column, flow rate 10 ml/min). The product was characterized by ESI-MS. The detected molecular ions were consistent with the calculated mass of **13** (2659.34). ESI-MS (+) m/z: found 1331.2 [$(M+2H)^{2+}$], 887.8 [$(M+3H)^{3+}$], 666.1 [$(M+4H)^{4+}$], 390.1 (fragment).

4.2.11. *O*-Acetyl deprotection of 13 (14)

The acetyl protected compound **13** was dissolved in dry methanol, cooled to 0 °C and hydrazine hydrate (1:6 v/v with methanol) was added slowly. The resulting reaction mixture was stirred at 0 °C for 30 min and then stirring was carried out at room temperature. The progress of the reaction was monitored by LC–ESI-MS. After 12 h, the reaction mixture was cooled to 0 °C and acetone was added slowly to achieve pH ~5. The organic solvents were removed in vacuo. The crude product was re-dissolved in water, lyophilized and purified by semi-preparative RP-HPLC using method 1 (Polaris 5 C_{18}-ether column, flow rate 10 ml/min). The obtained fractions were collected and solvents removed under vacuum, followed by dissolving the sample in ultra pure water and lyophilization. Ligand **14** was characterized by ESI-MS. The detected molecular ions were consistent with the calculated mass of **14** (2533.31). ESI-MS (+) m/z: found 1268.2 [$(M+2H)^{2+}$], 845.8 [$(M+3H)^{3+}$], 634.6 [$(M+4H)^{4+}$].

4.2.12. Preparation of the Gd^{3+} complex of ligand 14 (Gd-DOTA-k(FR)-Gal-CPP)

The concentration of ligand **14** was determined based on the absorbance of fluorophore. Ligand **14** (1 equiv) was dissolved in ultrapure water and a titrated solution of $GdCl_3$ (0.9 equiv) in water was added dropwise (pH was kept above 5.5 for the duration of the gadolinium addition). The pH was adjusted to 6–6.5 with 0.1 M NaOH. The solution was stirred at 40 °C for 12 h and then stirring was continued at room temperature for 3 days. The pH was checked periodically and adjusted to 6.5. The formation of Gd^{3+} complex was confirmed by analyzing aliquots of the reaction mixture by LC–ESI-MS. The crude product was purified by RP-HPLC, to remove ligand **14** and small impurities, using method 2 (Polaris C_8-Ether column, flow rate 4 ml/min) and afterwards dialyzed (Float-ALyser, cellulose ester membranes, MWCO 1000; Spectrum Laboratories Inc., Germany) and lyophilized to provide Gd-DOTA-k(FR)-Gal-CPP as yellow to orange solid. The detected molecular ions were consistent with the calculated mass of product (2688.21 g/mol).

The absence of free Gd^{3+} ions was verified in exemplary samples by a competitive assay with DTPA. The solution of **14** and $GdCl_3$ was stirred for 3 days and divided to two parts. One half was concentrated and purified by HPLC as described above. The second half was treated with excess of DTPA and stirred for additional 12 h and was subsequently purified by HPLC, dialyzed and lyophilized. No significant differences were observed in the relaxation rates R_1 measured at 123 MHz between both samples (equally concentrated) indicating the absence of free gadolinium in our CA after purification.

ESI-MS (−) m/z: found 2686.8 [$(M-H)^{1-}$], 1343.3 [$(M-2H)^{2-}$]; calcd for $C_{108}H_{173}GdN_{38}O_{31}S$ 2688.21. ESI-MS (+) m/z: found 1345.1 [$(M+2H)^{2+}$], 897.0 [$(M+3H)^{3+}$], 673.2 [$(M+4H)^{4+}$], 390 (FR).

4.2.13. Synthesis of Gd-DOTA-Gal-k(FR)-CPP

A side chain protected D-Tat_{49-57} (Fmoc-$r_{(Pbf)}k_{(Boc)}k_{(Boc)}r_{(Pbf)}r_{(Pbf)}q_{(Trt)}r_{(Pbf)}r_{(Pbf)}r_{(Pbf)}$) was synthesized on Fmoc/Pbf D-Arg preloaded Wang resin (0.08 mmol, 200 mg) using the same protocol as for conjugate **13**. The Fmoc group was then removed by treatment with 20% piperidine/DMF (2×) and resin was washed with DMF (4×). Next Fmoc-D-Lys-(Dde)-OH (4 equiv) pre-activated with HBTU (3.6 equiv)/HOBt (3.6 equiv) in DMF (2 ml) and DIPEA (8 equiv) were added and the reaction was stirred for 1 h. After Fmoc group deprotection, the monosaccharide **11** (3 equiv) was coupled to the lysine linker using HATU (3 equiv) and DIPEA (6 equiv) in DMF (3 ml). The reaction was completed after stirring for 3 h, as indicated by Kaiser test. The Fmoc group on the sugar residue was then deprotected and a solution of **12** (4 equiv) pre-activated with HATU (4 equiv) and DIPEA (8 equiv) in DMF (3 ml) was added to the resin. After stirring for 24 h, the resin was thoroughly washed with DMF and treated with 2% hydrazine hydrate in DMF (2 × 4 min). The ε-NH_2 of the lysine linker was reacted with FITC (4 equiv) and DIPEA (8 equiv) in DMF (3 ml) for 12 h. All coupling and deprotection steps were followed by a Kaiser test on the resin. The resin-bound conjugate was cleaved off by the procedure described for **13**. The acetate ester groups were deprotected according to the procedure described for **14**. The obtained ligand was purified by semi-preparative RP-HPLC and characterized by ESI-MS. The following preparation of Gd-DOTA-Gal-k(FR)-CPP was obtained using a protocol described for Gd-DOTA-k(FR)-Gal-CPP. The crude product was purified by RP-HPLC (Polaris C_8-Ether column, flow rate 4 ml/min) using method 2, dialyzed (48 h) and lyophilized to provide Gd-DOTA-Gal-k(FR)-CPP. Its structure was verified by ESI-MS. ESI-MS (+) m/z**:** found 1346.2 [$(M+2H)^{2+}$], 897.6 [$(M+3H)^{3+}$], 767.4 [$(M-FR)+3H)^{2+}$], 672.7 [$(M+4H)^{4+}$], 390 (FR fragment), calcd for $C_{108}H_{173}GdN_{38}O_{31}S$ 2688.21.

4.3. Concentration estimation

Fluorescein-labeled conjugates were dissolved in Milli-Q water to obtain a 10 mM solutions by weight and the pH was adjusted to ~7. To determine the real concentration of these stock solutions, the absorbance of a 1:100 dilution in Dulbecco's Modified Eagle's Medium (DMEM; Biochrom AG, Germany) was measured in a Fluostar Optima multiplate reader (BMG Labtech, Germany) at 485 nm with ratiometric correction of turbidity at 690 nm. The concentration of stock solutions was calculated assuming a molar extinction coefficient ($\varepsilon_{fluorescein}$) of 81,000 l/(mol cm). All further dilutions were done in proportion to the calculated concentration of the stock solutions.

4.4. Cell culture conditions

C6/LacZ cells (C6/lacZ7, ATCC® No.: CRL-2303™, USA) expressing β-galactosidase and C6 rat glioma cells (University of Tübingen, Germany) were cultured as monolayers at 37 °C in a 5% CO_2

humidified atmosphere in DMEM supplemented with 10% fetal bovine serum (FBS), 4 mM L-glutamine, 100 μg/ml streptomycin and 100 U/ml penicillin (all purchased from Biochrom AG, Germany). The culture medium of C6/LacZ cells was additionally supplemented with 0.1 mM non-essential amino acids (NEM, Biochrom AG, Germany). Both cell lines were passaged by trypsinization with trypsin/EDTA 0.05:0.02% (v/v) in phosphate-buffered saline (PBS; Biochrom AG, Germany) every second to third day.

4.5. Cellular uptake by fluorescence spectroscopy

C6 and C6/LacZ cells were grown in 96-well microplates. After reaching 70–80% confluence (24 h), cells were treated with different concentrations of Gd-DOTA-k(FR)-Gal-CPP in complete culture medium for 18 h under routine culture conditions. Subsequently, the supernatant was removed and the nuclear stain Hoechst 33342 (Hoe) in complete culture medium (100 μl/well) was added to cells in order to estimate their number per well (correlates to the DNA content).[57] After 30 min of incubation, cells were washed with Hank's buffered salt solution (HBSS; Biochrom AG, Germany), treated with cold trypan blue (TB) (0.05% (w/v) in PBS, 100 μl/well) for 3 min to quench extracellular fluorescence and repeatedly washed with HBSS. Cell-associated FR fluorescence (Ex 485 nm/Em 530 nm) and cell number based on Hoe fluorescence (Hoe, Ex 346 nm/Em 460 nm) were measured in the multiplate reader (Fluostar Optima, BMG Labtech, Germany). Cells incubated in the absence of Gd-DOTA-k(FR)-Gal-CPP were used as controls and wells without cells but treated with Hoechst, Trypan Blue and washed as described above were used as blanks. Hoe fluorescence was also used for the evaluation of cytotoxicity of CA. Experiments were run at least two times for each given concentration of Gd-DOTA-k(FR)-Gal-CPP with six replicates each.

4.6. Microscopy

Following fluorescence spectroscopy, microscopy on the same cells was performed without fixation using a Zeiss Axiovert 200 M microscope (Germany) with an LD Plan NeoFluor 40X objective. The conditions used for all imaging experiments were kept constant. Cellular localization of fluorescein linked conjugates was monitored by sample irradiation with blue light at 470 nm and observing emission at 525 nm. Hoechst-related fluorescence was viewed by excitation at 365 nm and emission at 460 nm. Trypan blue fluorescence was observed by irradiation at 535 and emission at 645 nm. Additionally, cell morphology was observed by capturing phase contrast images with differential interference contrast (DIC) microscopy of the same areas used for fluorescence detection. Volocity® Acquisition and Visualization software (Improvision/Perkin–Elmer, UK) was used for the image acquisition and processing.

4.7. MR imaging studies in cells

Exponentially growing C6/LacZ and C6 cells were incubated with 10 μM of Gd-DOTA-k(FR)-Gal-CPP in 175 cm^2 tissue culture flasks for 18 h at 37 °C. After washing twice with HBSS and once with PBS, cells were trypsinized and centrifuged. Cell viability was assessed by trypan blue staining. Subsequently, 2×10^7 cells, re-suspended in 500 μl of fresh complete culture medium without CA, were transferred to 1.5 ml Eppendorf tubes. Tubes with culture medium only and cells without CA in culture medium were used as controls. Before performing MR measurements, cells were allowed to settle in the tubes. Cell pellets were imaged at room temperature (~21 °C) with a clinical 3 T (123 MHz) human MR scanner (MAGNETOM Tim Trio, Siemens Healthcare, Germany), using a 12-channel RF Head coil and slice selective measurements from a slice with a thickness of 1 mm positioned through the cell pellet. Relaxation times (T_1) were measured using an inversion-recovery sequence, with an adiabatic inversion pulse followed by a turbo-spin-echo readout. Numbers of MR images acquired were in the range 10–15, with the time between inversion and readout varying from 23 to 3000 ms. With a repetition time of 10 s, 15 echoes were acquired per scan and averaged six times. All experiments scanned 256^2 voxels in a field-of-view of 110 mm in both directions resulting in a voxel volume of $0.43 \times 0.43 \times 1$ mm^3.

Data analysis was performed by fitting of relaxation curves with self-written routines under MATLAB 7.1 R14 (The Mathworks Inc., United States). The series of T_1 relaxation data were fitted to the following equation:

T_1 series with varying $t = T_I$:

$$S = S_0\ (1 - \exp(-t/T_I) + S(T_I = 0)\exp(-t/T_1).$$

Nonlinear least-squares fitting of three parameters S_0, $S_{(T_I=0)}$, and T_1 was done for manually selected regions of interest with the Trust-Region Reflective Newton algorithm implemented in MATLAB. The quality of the fit was controlled by visual inspection and by calculating the mean errors and residuals. The obtained T_1 values of the cell pellet were converted to $R_{1,\mathrm{cell}}$ (= $1/T_1$). These were expressed as % of control $R_{1,\mathrm{cell}}$ of cells incubated under the same conditions in the absence of CA.

4.8. Longitudinal relaxivity (r_1) of Gd^{3+} complexes

Relaxation times T_1 of aqueous solutions of Gd^{3+} complexes were determined at 123 MHz (3 T) and room temperature (~21 °C) as described above. Three to five samples with concentrations of Gd-DOTA-k(FR)-Gal-CPP (800 μl) in the range 5–40 μM were prepared in Milli-Q water. Pure water was used as a blank. Two times 200 μl of each sample were transferred to a 96-well plate and the absorbance was measured at 485 nm to evaluate the exact concentration of CA. Afterwards, samples for each concentration were combined again and 380 μl aliquots were transferred to Eppendorf cups for MR measurement (two replicates per concentration). Relaxation rate values were plotted on the exact concentration (in mM) and linear regression was done. The slope of the obtained curve showed the corresponding relaxivity.

4.9. Statistical analysis

Data are expressed as means ± standard error of the mean (SEM). Two mean values of interest were tested for statistically significant differences by unpaired student's *t*-test using GraphPad Prism version 5.02 for Windows (GraphPad Software, USA). When comparing more than two groups, a one-way analysis of variance (ANOVA) with Tukey's post-test for multiple comparisons was performed. *p*-values of <0.05 were considered statistically significant.

Acknowledgments

The authors thank Professor Hamprecht, University of Tübingen, for the kind gift of the C6 rat glioma cells. The authors are particularly grateful to Ms. Hildegard Schulz, High Field Magnetic Resonance Center, Max Planck Institute for Biological Cybernetics, for the help in performing the biological experiments. This work was funded by the Max Planck Society, supported by the German Ministry for Education and Research, BMBF (FKZ 01EZ0813), and was performed in the frame of COST action D38.

Supplementary data

Supplementary data associated with this article can be found, in the online version, at doi:10.1016/j.bmc.2011.03.023.

References and notes

1. Weissleder, R. *Radiology* **1999**, *212*, 609.
2. Navab, R.; Mort, J. S.; Brodt, P. *Clin. Exp. Metastasis* **1997**, *15*, 121.
3. Furumoto, S.; Takashima, K.; Kubota, K.; Ido, T.; Iwata, R.; Fukuda, H. *Nucl. Med. Biol.* **2003**, *30*, 119.
4. Bhaumik, S.; Gambhir, S. S. *Proc. Natl. Acad. Sci. U.S.A.* **2002**, *99*, 377.
5. Tung, C. H.; Zeng, Q.; Shah, K.; Kim, D. E.; Schellingerhout, D.; Weissleder, R. *Cancer Res.* **2004**, *64*, 1579.
6. Aime, S.; Botta, M.; Fasano, M.; Terreno, E. *Chem. Soc. Rev.* **1998**, *27*, 19.
7. Merbach, A. E.; Toth, E. *The Chemistry of Contrast Agents in Medical Magnetic Resonance Imaging*; John Wiley & Sons: Chichester, UK, 2001.
8. Louie, A. Y.; Huber, M. M.; Ahrens, E. T.; Rothbacher, U.; Moats, R.; Jacobs, R. E.; Fraser, S. E.; Meade, T. J. *Nat. Biotechnol.* **2000**, *18*, 321.
9. Querol, M.; Bennett, D. G.; Sotak, C.; Kang, H. W.; Bogdanov, A., Jr. *ChemBioChem* **2007**, *8*, 1637.
10. Nivorozhkin, A. L.; Kolodziej, A. F.; Caravan, P.; Greenfield, M. T.; Lauffer, R. B.; McMurry, T. J. *Angew. Chem., Int. Ed.* **2001**, *40*, 2903.
11. Hanaoka, K.; Kikuchi, K.; Terai, T.; Komatsu, T.; Nagano, T. *Chem. Eur. J.* **2008**, *14*, 987.
12. Duimstra, J. A.; Femia, F. J.; Meade, T. J. *J. Am. Chem. Soc.* **2005**, *127*, 12847.
13. Gilad, A. A.; Winnard, P. T., Jr.; van Zijl, P. C.; Bulte, J. W. *NMR Biomed.* **2007**, *20*, 275.
14. Huber, R. E.; Hlede, I. Y.; Roth, N. J.; McKenzie, K. C.; Ghumman, K. K. *Biochem. Cell Biol.* **2001**, *79*, 183.
15. Marshall, P.; Reed, C. G.; Sinnott, M. L.; Souchard, I. J. L. *J. Chem. Soc., Perkin Trans. 2* **1977**, 1198.
16. Bock, K.; Adelhorst, K. *Carbohydr. Res.* **1990**, *202*, 131.
17. Walovitch, R. C.; Hill, T. C.; Garrity, S. T.; Cheesman, E. H.; Burgess, B. A.; O'Leary, D. H.; Watson, A. D.; Ganey, M. V.; Morgan, R. A.; Williams, S. J. *J. Nucl. Med.* **1989**, *30*, 1892.
18. Janczuk, A. J.; Zhang, W.; Andreana, P. R.; Warrick, J.; Wang, P. G. *Carbohydr. Res.* **2002**, *337*, 1247.
19. Wacowich-Sgarbi, S. A.; Bundle, D. R. *J. Org. Chem.* **1999**, *64*, 9080.
20. Izumi, M.; Kaneko, S.; Yuasa, H.; Hashimoto, H. *Org. Biomol. Chem.* **2006**, *4*, 681.
21. Takaya, K.; Nagahori, N.; Kurogochi, M.; Furuike, T.; Miura, N.; Monde, K.; Lee, Y. C.; Nishimura, S. I. *J. Med. Chem.* **2005**, *48*, 6054.
22. Pietrzik, N. PhD Thesis, University of Tübingen, 2009.
23. Wei, W.; Tomohiro, T.; Kodaka, M.; Okuno, H. *J. Org. Chem.* **2000**, *65*, 8979.
24. Yan, L.; Kahne, D. *Synlett* **1995**, 523.
25. Qin, Z. H.; Li, H.; Cai, M. S.; Li, Z. J. *Carbohydr. Res.* **2002**, *337*, 31.
26. Mizukami, S.; Takikawa, R.; Sugihara, F.; Hori, Y.; Tochio, H.; Walchli, M.; Shirakawa, M.; Kikuchi, K. *J. Am. Chem. Soc.* **2008**, *130*, 794.
27. Lin, H.; Thayer, D. A.; Wong, C. H.; Walsh, C. T. *Chem. Biol.* **2004**, *11*, 1635.
28. Kunz, H.; Unverzagt, C. *Angew. Chem., Int. Ed. Engl.* **1988**, *27*, 1697.
29. Brocke, C.; Kunz, H. *Synthesis-Stuttgart* **2004**, 525.
30. Sjolin, P.; Elofsson, M.; Kihlberg, J. *J. Org. Chem.* **1996**, *61*, 560.
31. Abiraj, K.; Jaccard, H.; Kretzschmar, M.; Helm, L.; Maecke, H. R. *Chem. Commun. (Camb.)* **2008**, 3248.
32. De Leon-Rodriguez, L. M.; Ortiz, A.; Weiner, A. L.; Zhang, S.; Kovacs, Z.; Kodadek, T.; Sherry, A. D. *J. Am. Chem. Soc.* **2002**, *124*, 3514.
33. Rohrer, M.; Bauer, H.; Mintorovitch, J.; Requardt, M.; Weinmann, H. J. *Invest. Radiol.* **2005**, *40*, 715.
34. Caravan, P. *Chem. Soc. Rev.* **2006**, *35*, 512.
35. Caravan, P.; Farrar, C. T.; Frullano, L.; Uppal, R. *Contrast Media Mol. Imaging* **2009**, *4*, 89.
36. Fulton, D. A.; Elemento, E. M.; Aime, S.; Chaabane, L.; Botta, M.; Parker, D. *Chem. Commun. (Camb.)* **2006**, 1064.
37. Snyder, E. L.; Dowdy, S. F. *Pharm. Res.* **2004**, *21*, 389.
38. El-Andaloussi, S.; Jarver, P.; Johansson, H. J.; Langel, U. *Biochem. J.* **2007**, *407*, 285.
39. Rennert, R.; Wespe, C.; Beck-Sickinger, A. G.; Neundorf, I. *Biochim. Biophys. Acta* **2006**, *1758*, 347.
40. Gump, J. M.; Dowdy, S. F. *Trends Mol. Med.* **2007**, *13*, 443.
41. Brooks, H.; Lebleu, B.; Vives, E. *Adv. Drug Delivery Rev.* **2005**, *57*, 559.
42. Abes, S.; Williams, D.; Prevot, P.; Thierry, A.; Gait, M. J.; Lebleu, B. *J. Controlled Release* **2006**, *110*, 595.
43. Tripathi, S.; Chaubey, B.; Ganguly, S.; Harris, D.; Casale, R. A.; Pandey, V. N. *Nucleic Acids Res.* **2005**, *33*, 4345.
44. Bullok, K.; Piwnica-Worms, D. *J. Med. Chem.* **2005**, *48*, 5404.
45. Vocero-Akbani, A. M.; Heyden, N. V.; Lissy, N. A.; Ratner, L.; Dowdy, S. F. *Nat. Med.* **1999**, *5*, 29.
46. Prantner, A. M.; Sharma, V.; Garbow, J. R.; Piwnica-Worms, D. *Mol. Imaging* **2003**, *2*, 333.
47. Allen, M. J.; Meade, T. J. *J. Biol. Inorg. Chem.* **2003**, *8*, 746.
48. Terreno, E.; Crich, S. G.; Belfiore, S.; Biancone, L.; Cabella, C.; Esposito, G.; Manazza, A. D.; Aime, S. *Magn. Reson. Med.* **2006**, *55*, 491.
49. Geninatti Crich, S.; Cabella, C.; Barge, A.; Belfiore, S.; Ghirelli, C.; Lattuada, L.; Lanzardo, S.; Mortillaro, A.; Tei, L.; Visigalli, M.; Forni, G.; Aime, S. *J. Med. Chem.* **2006**, *49*, 4926.
50. El-Andaloussi, S.; Johansson, H. J.; Lundberg, P.; Langel, U. *J. Gene Med.* **2006**, *8*, 1262.
51. Raagel, H.; Saalik, P.; Pooga, M. *Biochim. Biophys. Acta* **2010**, *1798*, 2240.
52. Cheung, J. C.; Kim Chiaw, P.; Deber, C. M.; Bear, C. E. *J. Controlled Release* **2009**, *137*, 2.
53. Pawley, J. B. *Handbook of Biological Confocal Microcopy*, 3rd ed.; Springer: NY, 2006.
54. Raty, J. K.; Liimatainen, T.; Kaikkonen, M. U.; Grahn, O.; Airenne, K. J.; Yla-Herttuala, S. *Mol. Ther.* **2007**, *15*, 1579.
55. Ugurbil, K.; Jha, D.; Engelmann, J.; Mishra, R.; Wiesmüller, K.-H. WO/2009/100934, 2009.
56. Gottlieb, H. E.; Kotlyar, V.; Nudelman, A. *J. Org. Chem.* **1997**, *62*, 7512.
57. Blaheta, R. A.; Franz, M.; Auth, M. K.; Wenisch, H. J.; Markus, B. H. *J. Immunol. Methods* **1991**, *142*, 199.